

Equine Podotrochlear Apparatus - Histologic Characterization

Grasiela De Bastiani¹, Flávio Desessards De La Côte², Adriano Tony Ramos¹,
Tainã Kuwer Jacobsen¹, Glaucia Denise Kommers² & Malcon Andrei Martinez-Pereira¹

ABSTRACT

Background: The navicular syndrome may be associated with alterations in other podotrochlear apparatus components, such as the deep digital flexor tendon, collateral sesamoid and distal sesamoid ligaments, podotrochlear bursa and distal sesamoid bone. However, the clinical significance and nature of these changes are not well understood, many of descriptive reports about distal sesamoid bone lesions are rarely accompanied by a complete and comprehensive comparison with animals of the control group. The aim of this study was to describe histologically findings of the podotrochlear apparatus components, allowing the understanding of the inserts and their microscopic appearance, thus providing the future recognition of their alterations.

Materials, Methods & Results: Fourteen samples of the podotrochlear apparatus were taken out of 44 equine thoracic limbs specimens, separated at the radiocarpal joint of Crioulo and Thoroughbred horses, with an average age of 6.0-year-old, coming from a private clinic in southern Brazil. The thoracic limbs specimens were refrigerated at 4°C at the clinic and then they were sent to the University Federal of Santa Maria (UFSM). Once at the University laboratory, the specimens were dissected to isolate the podotrochlear apparatus from each one. Subsequently, transversal and longitudinal samples from the distal sesamoid bone, deep digital flexor tendon, distal sesamoid ligament, collateral sesamoid ligament, were collected and podotrochlear bursa which were processed at the Veterinary Pathology Laboratory of the UFSM and University Federal of Santa Catarina (UFSC). The tissues samples were fixed in a 10% formaldehyde solution for 14 days and routinely processed for histology. The samples were sectioned at 3 µm and stained using the hematoxylin-eosin (H-E) routine method. The bone samples, after fixation, underwent a decalcified process in a formic acid-sodium citrate aqueous solution and routinely processed for histopathology. Histologic tendons evaluation showed that it is arranged in honeycombs fascicles in a transverse section observation. The tendinous fibers have a more compact and aligned collagen fibers arrangement due to the dense connective tissue. The synovial membrane of the podotrochlear bursa is composed of a cubic pseudo conjunctival epithelium arranged with a layer of synoviocytes forming villi towards the lumen. This characterization is very similar to that of the synovial joint membrane. The collateral sesamoid ligament fibers are not perfectly aligned, occurring at their confluence in some areas accompanied by the dissection of adipose tissue. The distal sesamoid ligament fibers, composed by of loose connective tissue associated with synoviocytes and vascular stroma. The articular surface of the distal sesamoid bone is arranged in 3 layers of chondrocytes embedded in a hyaline matrix. There was a clear differentiation between the subchondral bone area and the fibrocartilage tissue in the palmar aspect of the distal sesamoid bone.

Discussion: The morphophysiological characterization of the podotrochlear structures inside the hoof capsule it is important for the future recognition of abnormalities and the possible hypothesis that originates the podotrochlear syndrome. These changes have great clinical relevance and very often associated of distal limb lameness in horses. The normal macroscopic, ultrasonographic and radiographic images along with the histomorphometric study of the podotrochlear structures have contributed for the morphophysiological comprehension and consequently future interpretation of the podotrochlear structures diseases.

Keywords: podotrochlear apparatus, distal sesamoid bone, deep digital flexor tendon, navicular syndrome, histological findings.

DOI: 10.22456/1679-9216.119100

Received: 6 October 2021

Accepted: 20 December 2021

Published: 12 January 2022

¹Universidade Federal de Santa Catarina (UFSC), Curitibaanos, SC, Brazil. ²Universidade Federal de Santa Maria (UFSM), Santa Maria, RS, Brazil. CORRESPONDENCE: T.K. Jacobsen [tainajacobsen@gmail.com]. UFSC. Rodovia Ulysses Gaboardi km 3. CEP 89520-000 Curitibaanos, SC, Brazil.

INTRODUCTION

The coexistence of lesions in the navicular or distal sesamoid bone (DSB) and in the deep digital flexor tendon (DDFT) and other components of the podotrochlear apparatus, such as collateral sesamoid ligament (CSL), distal sesamoid ligament (DSL) and the podotrochlear bursa (PtB) is reported [6]. However, the clinical significance and nature of these changes are not well understood, and it is proposed that navicular diseases are related to fibrocartilaginous degeneration of vascular origin [18]. However, many of descriptive reports about distal sesamoid bone lesions are rarely accompanied by a complete and comprehensive comparison with animals of the control group [19].

The DSB is a central component of the podotrochlear apparatus, that significantly absorbs the impact during the suspension and flexion phases of the stride. The function of the DSB is to promote a constant angle for the insertion of the DDFT, which follows the palmar / plantar aspect of this bone. This is related to its fibrocartilaginous surface, that facilitating the sliding effect during of the locomotion phases [21]. In fact, a histological study, different structures were characterized as part of the navicular disease including synovial membrane, DSL, CSL and DDFT [3].

The aim of this study was to described histologically findings of the podotrochlear apparatus components, allowing the understanding of the inserts and their microscopic appearance, thus providing the future recognize of their alterations.

MATERIALS AND METHODS

Collection of the specimens

Fourteen samples of the podotrochlear apparatus were taken out of 44 equine thoracic limbs (TL) specimens, separated at the radiocarpal joint of Crioulo and Thoroughbred horses, with an average age of 6.0-year-old, coming from a private clinic in southern Brazil, located 139 m of altitude, and latitude: 29° 41' 29" south and longitude: 53° 48' 3" west. The TL specimens were refrigerated at 4°C at the clinic and then they were sent to the University Federal of Santa Maria (UFSM). Once at the University laboratory, the specimens were dissected to isolate the podotrochlear apparatus from each one. Subsequently, transversal and longitudinal samples from the DSB, DDFT, DSL, CSL were collected and PtB which were processed at

the Veterinary Pathology Laboratory of the UFSM and University Federal of Santa Catarina (UFSC).

Preparation of the samples

The tissues samples were fixed in a 10% formaldehyde solution for 14 days and routinely processed for histology. The samples were sectioned at 3 µm and stained using the hematoxylin-eosin¹ (HE) routine method. The bone samples, after fixation, underwent a decalcified process in a formic acid-sodium citrate aqueous solution and routinely processed for histopathology.

The DDFT was sectioned proximal to the PtB and CSL. The CSL was collected proximal to the PtB in its contact with the DDFT, while the PtB was sectioned proximally to the DSB. The bulbs of the heels and frog were removed to allow entire exposure of the DSB and DSL allowing access to these structures to collect samples.

Inclusion criteria

The inclusion criteria for this study were based on the absence of radiographic and contrasted PtB, ultrasound and macroscopic abnormalities in the equine TL specimens related to the podotrochlear apparatus components. In addition, samples with histopathological changes such as cartilaginous metaplasia, fibroplasia and neovascularization of tendons and ligaments were discarded. For the distal sesamoid bone, abnormalities in the cortical and subchondral layer were removed from the present study.

The samples of the equine podotrochlear apparatus were microscopically observed and divided as: DDFT (n = 4; 28.57%), PtB (n = 2; 14.28%), CSL (n = 2; 14.28%), DSB (n = 4; 28.57%) and DSL (n = 2; 14.28%).

RESULTS

Deep digital flexor tendon (DDFT)

In a longitudinal suprasesamoid section, was possible to observe the linear arrangement of tendon fibers paralleled arranged by a dense connective tissue. This arrangement was interspersed by the nucleus of the elongated cells distributed in a uniform and perpendicular way (Figure 1). In addition, convoluted blood vessels were identified accompanying the tendon fibers, when the tendon carries out elastic movements. This tortuousness of blood vessels does not characterize part of the healing process, as fibroplasia (Figure 2). In a transversal section, the tendon fascicles arrangement

was delimited by a dense non-modeled connective tissue, rich in blood vessels and stroma (Figure 3). In contrast, in the distal sesamoid region, the fibers adopt a slightly wavy, elongated, and well-defined arrangement and their parallelism is not expressed with the same intensity as the suprasesamoid region, being accompanied by a developed dense connective tissue that corresponds to the peritendon. The peritendon, in a longitudinal histological section, is characterized by a dense connective tissue not modeled, with a large concentration of blood vessels in a cubic epithelium.

Podotrochlear bursa (PtB)

The PtB, in the sesamoid region, was dissected from its intimate contact with the DDFT (Figures 4 &

5) and it was evaluated in a cross section where it was observed that the PtB is surrounded by 3 layers of cubic conjunctival pseudo epithelium in the lumen, arranged by oval shape cells interspersed by a vascular stroma composed of loose connective tissue, characterizing a synovial membrane (Figure 6). This structure corresponds to the PtB with its villi and the tortuosity of its blood vessels that converge towards the lumen. The superficial layer has an intensely basophilic matrix, being regular and thin throughout its course. In some histological sections, it was observed the presence of adipose tissue separating the DDFT and the PtB, as well as, it was verified the dissection of stroma and cubital pseudo epithelium separating the tendinous fibers of this.

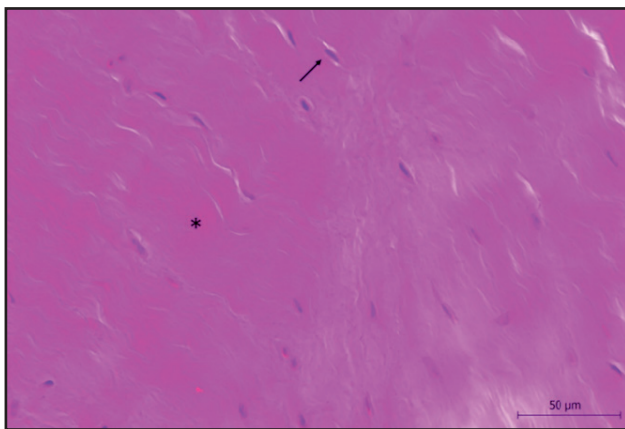


Figure 1. Longitudinal section of DDFT: paralleled arrangement of collagen fibers (asterisk); elongated cells called tenocytes (arrow). [HE; Bar= 40 µm].

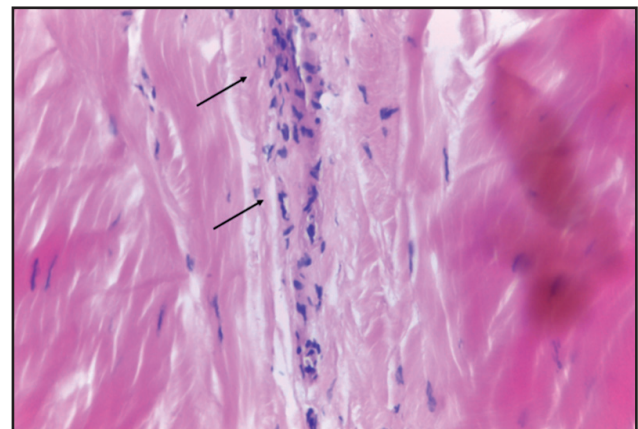


Figure 2. Longitudinal section of DDFT: vessels tortuosity (arrows). [HE; Bar= 40 µm].

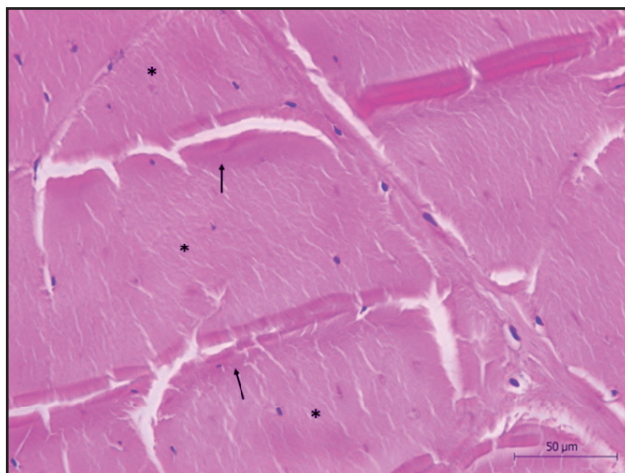


Figure 3. Transverse section of the DDFT: honeycomb arrangement fascicles (asterisks) delimited by non modeled dense connective tissue (arrows). [HE; Bar= 40 µm].

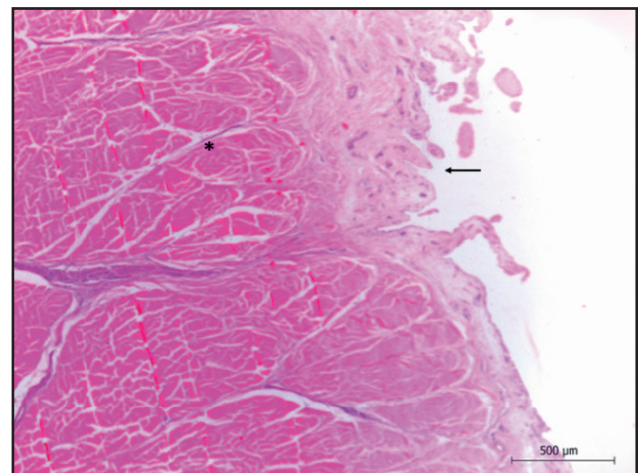


Figure 4. Transverse section of the DDFT and podotrochlear bursa: intimate contact of the DDFT honeycomb fascicles (asterisk) and podotrochlear bursa (arrow) in the supra sesamoidean region. [HE; Bar= 10 µm].

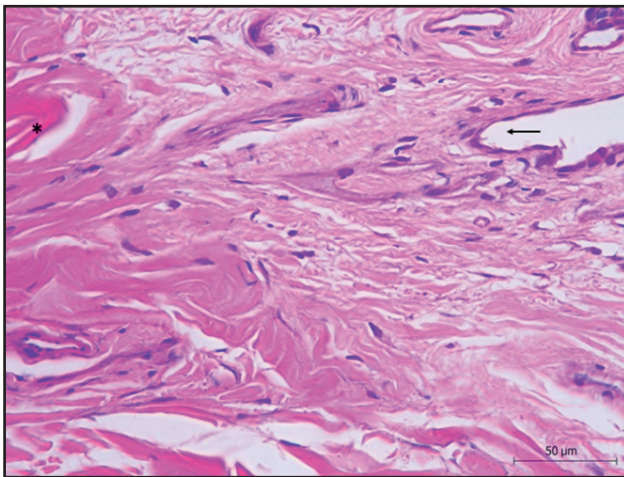


Figure 5. Transverse section of the DDDFT and podotrochlear bursa- observed the intimate contact of the DDDFT honeycomb fascicles (asterisk) and podotrochlear bursa (arrow) in the supra sesamoidean region. Stained hematoxylin and eosin. [HE; Bar = 10 μm].

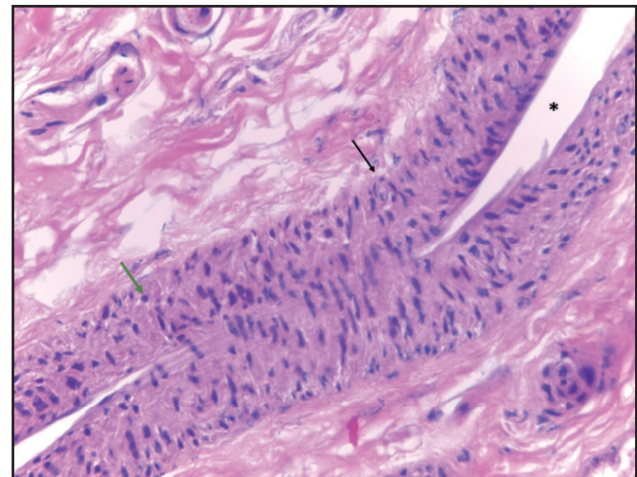


Figure 6. Longitudinal section of podotrochlear bursa: the synovial membrane arranged in 3 layers (black arrow) composed by synoviocytes (green arrow) running for the lumen (asterisk). [HE; Bar= 40 μm].

Collateral sesamoid ligament (CSL)

In a longitudinal section, it was observed that the CSL had a wavy arrangement of fibers right at the intimate contact with the PtB, characterized by bundles of dense connective tissue interspersed by the vascular stroma of the PtB (Figure 7). The ligament fibers are moderately packed by a dense connective tissue interspersed in their insertion into the DSB by a hyaline matrix and some dispersed chondrocytes. Additionally, these fibers are not perfectly arranged, with their confluence occurs in some regions and may be accompanied by the dissection of an adipose connective tissue. Fibroblasts were thin and characteristic, and follow the wavy arrangement of ligament fibers (Figure 8).

Distal sesamoid bone (DSB)

The articular surface of the DSB which is in intimate contact with the third phalanx is arranged in 3 layers of chondrocytes imbedded in a hyaline matrix, like what is observed in sections from another arthroial joint (Figure 9). The superficial articular layer has a regular and basophilic appearance. However, as more distant of the joint surface, they become oval shaped and arranged in groups, which is usually observed in doubles. Nearby the spongy layer, the chondrocytes are dispersed and showed a circular shape. Clearly, the subchondral layer is characterized by being more compact, hyaline, rich in osteocytes with its blood vessels, Haversian and

Volkman canals (Figure 10). Below the subchondral bone we find the spongy bone, characterized by a trabecular tissue formed in some points by immature osteocytes and filled with adipose tissue (Figure 11). In the transition between the subchondral and spongy layers, there are eosinophilic lines interspersed with basophilic lines. Probably this is the local where the differentiation of mineral deposition occurred. On the flexor and/or fibrocartilaginous surface, a hyaline matrix interspersed with isolated and highly stained chondrocytes is observed, associated with the presence of collagen fibers of the CSL, in the proximal portion, and of the DSL, distally, both intimately attached to the bone surface.

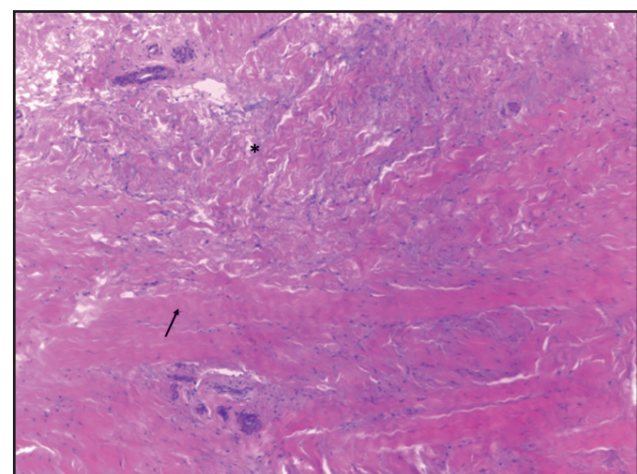


Figure 7. Longitudinal section of the collateral sesamoid ligament: intrinsic contact of podotrochlear bursar vascular stroma (asterisk) with collateral sesamoid ligament collagen fibers (arrow). [HE; Bar= 40 μm].

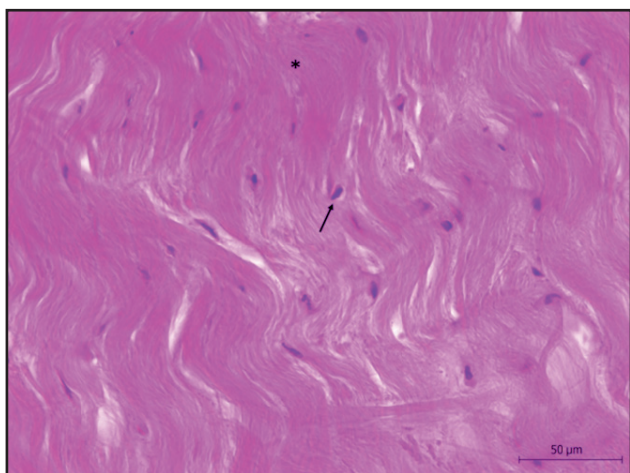


Figure 8. Longitudinal section of the collateral sesamoid ligament: wave arrangement of ligament collagen fiber (asterisk) interspersed by fibroblast cells called desmocytes (arrow). [HE; Bar= 40 µm].

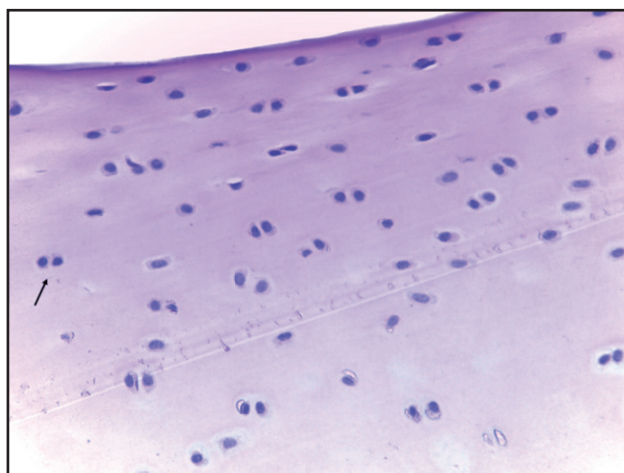


Figure 9. Transverse section of the distal sesamoid bone: condrocytes disposed in 3 layers embedded in hyaline matrix cartilage (arrow). [HE; Bar= 40 µm].



Figure 10. Transverse section of the distal sesamoid bone: transition of the articular cartilage (arrow) and subchondral bone (asterisk). [HE; Bar= 40 µm].

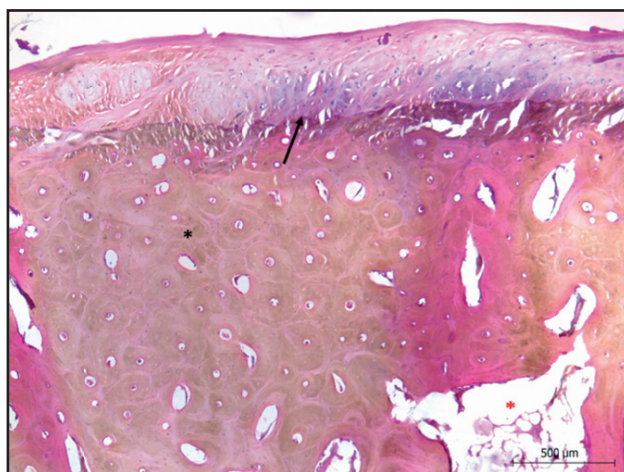


Figure 11. Transverse section of the distal sesamoid bone - observed the clearly differentiation of the articular cartilage (arrow), subchondral bone (black asterisk) and trabecular bone (red asterisk). Stained hematoxylin and eosin. [HE; Bar = 10 µm].

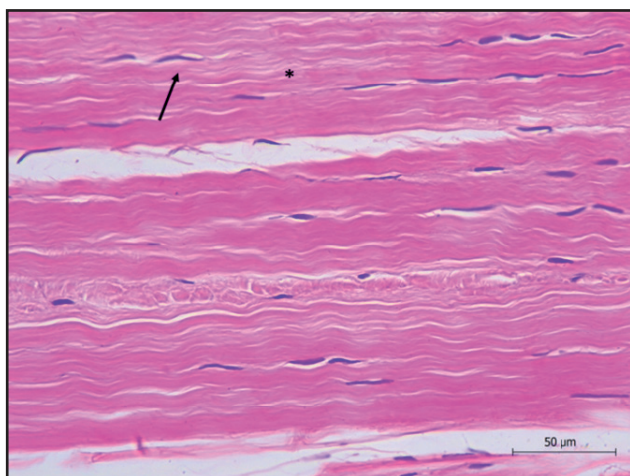


Figure 12. Longitudinal section of the distal sesamoid ligament: collagen fibers undulating arrangement (asterisk) interspersed by elongated cells called desmocytes (arrow). [HE; Bar= 40 µm].

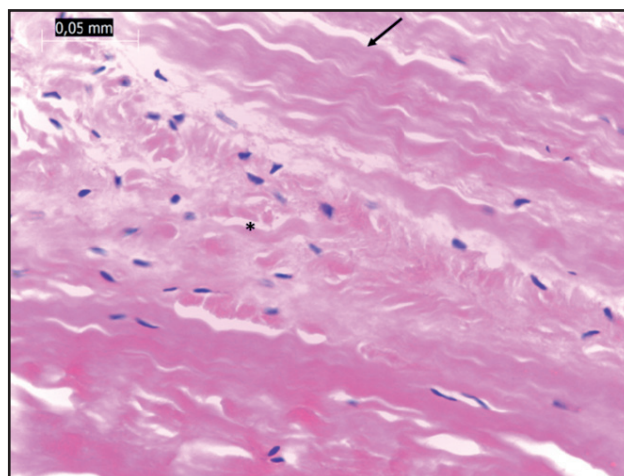


Figure 13. Longitudinal section of the distal sesamoid ligament: podotrochlear bursa vascular stroma (asterisk) dissected the collagen wave ligament fibers (arrow). [HE; Bar= 40 µm].

Distal sesamoid ligament (DSL)

The collagen fibers of the DSL sectioned between the insertion in the DSB and in the third phalanx have a slightly waving arrangement perfectly disposed and delimited in a longitudinal section (Figure 12). The collagen fibers are not densely packed by connective tissue, but, in contrast, they have a loose appearance interspersed by some reticular basophilic fibers. In addition, in some samples, the dissection of ligament fibers was identified by an organized loose tissue interspersed by synoviocytes and vascular stroma, which may possibly be associated with the tissue of the PtB, thus promoting a connection between the DDFT and the sesamoid ligament (Figure 13).

DISCUSSION

The inclusion criteria used in this study was the absence of macroscopic, radiographic (including a PtB contrast study), ultrasonographic abnormalities, in addition to the absence of history of lameness referred to the podotrochlear apparatus. The morphophysiological characterization of the podotrochlear structures inside the hoof capsule such as DDFT, PtB, CSL, DSB and DSL it is important for the future recognition of abnormalities and the possible hypothesis that originates the podotrochlear syndrome. These changes have great clinical relevance and very often associated of distal limb lameness in horses.

According to Dyson *et al.* [6] foreground the coexistence of lesions in the DDFT and SDB, and other components of podotrochlear apparatus such as PtB, CSL and DSL. These diseases may be directly related to a chronic response to excessive stress of the podotrochlear apparatus. Biomechanics distal thoracic limbs studies demonstrated that the greatest forces applied to the podotrochlear apparatus area is during the propulsion phase of the walking, due to the increased tension in the DDFT on the flexor surface of the distal DSB and a wide contact between the second phalanx, increasing consequently the tension in the CSL [7]. Therefore, the coexistence of podotrochlear apparatus lesions is not surprising, thus intensifying histology studies for better characterization of these structures, insertion areas and entheses.

At the macroscopic evaluation, the tendons are constituted by linear collagen fibers arranged in colourless reticulate fibrous bundles in continuity to the dorsal surface of the tendon. Histology evaluation

of the tendons showed that it is organized in honeycombs called fascicles in a transverse orientation. Larger blood vessels were observed on the palmar surface of this structure and cartilaginous metaplasia at the DDFT distal insertion [5]. Some collagen ligamentous fibers were found on the DSB flexor palmar surface associate with isolated chondrocytes in some areas. Such an event perhaps constitutes a transition area between the CSL and the fibrocartilaginous tissue of the navicular bone. Adhesions between the DDFT and SDB palmar surface area are often associated with erosions of palmar fibrocartilage and fibrillation of the dorsal surface of the DDFT [20]. The tendinous fibers of the DDFT have a more compact and aligned collagen fibers arrangement due to the dense connective tissue; it contrasts with the fibroplasia which is characterized by a disorganized loose connective tissue [10].

The podotrochlear bursa adhesions occurred between the DDFT, CSL, DSB palmar surface area and DSL. The prevalence of fibrous adhesions in racehorses with clinical navicular disease is unknown, however a study has shown that they were present between DDFT and SDB in 34% of racehorses with clinical navicular disease. In this same experimental model, adhesions were not observed in horses without this clinical presentation [22]. Histologic observation in this research work demonstrated that the PtB synovial membrane is made of a cubic pseudo conjunctival epithelium arranged with a layer of synoviocytes forming villi towards the lumen. This characterization is very similar to the synovial joint membrane. The synovial membrane is in intimate contact with the palmar surface of the joint capsule and it is characterized by being an extremely thin, light pink colour structure, and the synoviocytes are concentrated along its entire length [9]. Observed in the PtB histologic sections a lumen delimited by as layers with the synovial fluid. The synovial fluid inside the PtB allows a clear outline of the podotrochlear apparatus structures [15]. In normal conditions the synovial fluid is present in the PtB and represents an important finding in the ultrasonographic images. Navicular bursitis abnormalities includes presence of increased synovial fluid, severe thickening associate with scar tissue formation and adhesions areas of the PtB [17].

The SCL is arranged symmetrically and, forming a fibroblastic structure like a collar shape running from the dorsal surface of the collateral

ligament of the proximal interphalangeal joint, and also the middle phalanx proceeding this final insertion to the DSB acting as a support of this structure. In addition, it contributes to the formation of distal scutum along with the DSB, and these ligament fibers continuity with the collateral ligament of the proximal interphalangeal joint [1]. Histologically, the ligamentous collagen fibers are arranged in parallel waves [9]. However, little is known about the adherences between DDFT, SCL, DSL [4]. In this study was observed that the fibers of the SCL are not perfectly aligned, occurring at their confluence in some areas accompanied by the dissection of adipose connective tissue.

Lameness attributed to the podotrochlear apparatus are associated with abnormalities involving a variety of structures [14], but frequently are primarily located in bones, tendons, ligaments and synovial structures [7]. Such abnormalities of the DSB included distal and proximal enthesopathies, distal surfaces fragments, shape and increased numbers of synovial invaginations in the distal border, irregularities of the endosteal surface compromising the compact bone and fibrocartilage eburnation in the palmar surface [11]. The articular and dorsal surface of the DSB is in close contact with the distal phalanx and characterized by chondrocyte layers submerged in a hyaline matrix. Above the subchondral bone, 3 articular cartilage layers may be identified, such as a deep layer delimits the subchondral bone with the chondrocytes have a vertical arrangement and radial shape of collagen fibers. Voluminous chondrocytes and collagen fibers are randomly oriented in the intermediated layer and superficial layer presented the ovoid chondrocytes shape and tangentially collagen fibers [9]. The subchondral portion of the DSB is rich in osteocytes and delimited from the trabecular portion by adipocytes tissue. In radiographic observation without navicular disease, it is easily differentiated in a lateromedial projection the

radiopacity of subchondral bone and the radiolucency of the trabecular bone [8]. The palmar aspect of the DSB corresponding to the flexor surface and, in this study it was observed a clear differentiation between the subchondral bone area and fibrocartilage tissue.

The DDFT and DSL insertion in the distal phalanx is characterized by a dense connective tissue separated by a loose connective tissue, associated with a small arteriovenous complex, elastic tissue and a large sensory nerve fibers [2]. Thin septa of connective tissue were observed between the DDFT and the DSL demonstrated that improbable direct contact of the synovium the PtB with the DSB and remote responsible for resorptive lesions [23]. It was observed the presence of loose connective tissue associated with synoviocytes and vascular stroma when dissecting the DSL fibers. The DSL is characterized by 3-4 mm and, that is more echogenic in comparison to the DDFT. A thin anechoic structure is observed between the DSL and DDFT that corresponds to the synovial membrane of the PtB [12,16]. The linear anechoic area between DSL and DDFT was described in a study in 79.2% of horses and was found in both sides in 63.1% in horses that did not presented podotrochlear clinical diseases [13].

CONCLUSION

The normal macroscopic, ultrasonographic and radiographic images along with the histomorphometric study of the podotrochlear structures have contributed for the morphophysiological comprehension and consequently future interpretation of the podotrochlear structures diseases.

MANUFACTURER

¹Êxodo Científica. Sumaré, SP, Brazil.

Declaration of interest. The authors report no conflicts of interest. The authors alone are responsible for the content and writing of this article.

REFERENCES

- 1 **Barone R. 1989.** Articulations metacarpo-phalangiennes. In: *Anatomie Comparée des Mammifères Domestiques - Tome 2: Arthrologie et Myologie*. Paris: Vigot, pp.187-204.
- 2 **Bowker R.M., Atkinson P.J., Atkinson T.S. & Haut R.C. 2001.** Effect of contact stress in bones of the distal interphalangeal joint on microscopic changes in articular cartilage and ligaments. *American Journal of Veterinary Research*. 62: 414-424.
- 3 **Blunden A., Dyson S., Murray R. & Schramme M. 2006.** Histopathology in horses with chronic palmar foot pain and age-matched controls. Part 1: Navicular bone and related structures. *Equine Veterinary Journal*. 38: 15-22.

- 4 Blunden A., Murray R. & Dyson S. 2009. Lesions of the deep digital flexor tendon in the digit: a correlative MRI and post-mortem study in control and lame horses. *Equine Veterinary Journal*. 41: 25-33.
- 5 Busoni V., Snaps F., Trenteseaux J. & Dondelinger R.F. 2004. Magnetic resonance imaging of the palmar aspect of the equine podotrochlear apparatus: normal appearance. *Veterinary Radiology & Ultrasound*. 45(3): 198-204.
- 6 Dyson S., Murray R., Blunden T. & Schramme M. 2006. Current thoughts on the pathogenesis of navicular disease. *Equine Veterinary Education*. 18: 45-56.
- 7 Dyson S. & Murray R. 2007. Magnetic resonance imaging evaluation of 264 horses with foot pain: The podotrochlear apparatus, deep digital flexor tendon and collateral ligaments of the distal interphalangeal joint. *Equine Veterinary Journal*. 39(4): 340-343.
- 8 De Zani D., Polidori C., Di Giancamillo M. & Zani D.D. 2016. Correlation of radiographic measurements of structures of the equine foot with lesions detected on magnetic resonance imaging. *Equine Veterinary Journal*. 48: 165-171.
- 9 De Bastiani G., De La Corte F.D., Kommers G.D., Brass K.E., Pereira R., Cantarelli C. & Silva M.T. 2017. Aspectos ultrassonográficos, anatômicos e histológicos normais da articulação metacarpofalangeana equina. *Pesquisa Veterinária Brasileira*. 37(10):1165-1171.
- 10 De Bastiani G., De La Corte F.D., Brass K.E., Cantarelli C., Dau S., Kommers G.D., Silva M.T. & Silva A.M. 2018. Histochemistry of equine damage tendons, ligaments and articular cartilage. *Acta Scientiae Veterinariae*. 46: 1612. 8p.
- 11 Holowinski M.E., Solano M., Maranda L. & Garcia Lopez J.M. 2012. Magnetic resonance imaging of navicular bursa adhesions. *Veterinary Radiology & Ultrasound*. 53(5): 566-572.
- 12 Jacquet S. & Denoix J. 2012. Ultrasonographic examination of the distal podotrochlear apparatus of the horse: A trans cuneal approach. *Equine Veterinary Education*. 24: 90-96.
- 13 Kristoffersen M. & Thoenen M.B. 2003. Ultrasonography of the navicular region in horses. *Equine Veterinary Education*. 15: 150-157.
- 14 Murray R., Blunden T., Schramme M. & Dyson S. 2006. How does magnetic resonance imaging represent histological findings in the equine digit? *Veterinary Radiology & Ultrasound*. 47: 17-31.
- 15 Maher M.C., Werpy N.M., Goodrich L.R. & McIlwraith C.W. 2011. Positive contrast magnetic resonance burrography for assessment of the navicular bursa and surrounding soft tissues. *Veterinary Radiology & Ultrasound*. 52: 385-393.
- 16 MacDonald J.L., Richter R.A. & Wimer C.L. 2018. Ultrasonographic variations are present in the distal sesamoidean impar ligament f clinically sound horses. *Veterinary Radiology & Ultrasound*. 59: 607-612.
- 17 Marsh C. 2016. MRI in the diagnosis of foot lameness and therapeutic approaches following an accurate MRI diagnosis. In: *Proceedings of the 62nd Annual Convention of the American Association of Equine Practitioners - AAEP* (Orlando, USA). pp.138-148.
- 18 Pool R.R., Meagher D.M. & Stover S.M. 1989. Pathophysiology of Navicular Syndrome. *Veterinary Clinics of North America: Equine Practice*. 5(1): 109-129.
- 19 Rijkenhuizen A.B.M., NBmeth F., Dik K.J. & Goedegebuure S.A. 1989. The arterial supply of the navicular bone in adult horses with navicular disease. *Equine Veterinary Journal*. 21: 418-424.
- 20 Sherlock C., Mair T. & Blunden T. 2008. Deep erosions of the palmar aspect of the navicular bone diagnosed by standing magnetic resonance imaging. *Equine Veterinary Journal*. 40: 684-692.
- 21 Waguespack R. & Hanson R. 2010. Navicular syndrome in equine patients: anatomy, causes, and diagnosis. *Compendium: Continuing Education for Veterinarians*. 32(12): E7. pp.1-14.
- 22 Wright I.M., Kidd L. & Thorp B.H. 1998. Gross, histological, and histomorphometric features of the navicular bone and related structures in the horse. *Equine Veterinary Journal*. 30: 220-234.
- 23 Van Wulfen K.K. & Bowker R.M. 2002. Microanatomic characteristics of the insertion of the distal sesamoidean impar ligament and deep digital flexor tendon on the distal phalanx in healthy feet obtained from horses. *American Journal of Veterinary Research*. 63: 215-221.